Lunar Gruithuisen and Mairan domes: Rheology and mode of emplacement

Lionel Wilson
Environmental Science Department, Lancaster University, Lancaster, United Kingdom

James W. Head
Department of Geological Sciences, Brown University, Providence, Rhode Island, USA

Received 1 April 2002; revised 10 October 2002; accepted 20 November 2002; published 26 February 2003.

[1] The lunar steep-sided Gruithuisen and Mairan domes are morphologically and spectrally distinctive structures and appear similar to terrestrial extrusive volcanic features characterized by viscous magma. We use the basic morphologic and morphometric characteristics of the domes to estimate the yield strengths ($\sim 10^5$ Pa), plastic viscosities ($\sim 10^9$ Pa s), and effusion rates (~ 50 m^3/s) of the magmas which formed them. These values are similar to those of terrestrial rhyolites, dacites, and basaltic andesites and support the hypothesis that these domes are an unusual variation of typical highlands and mare compositions. The dikes which formed them are predicted to have had widths of ~ 50 m and lengths of about 15 km. The magma rise speed implied by this geometry is very low, $\sim 7 \times 10^{-5}$ m/s, and the Reynolds number of the motion is $\sim 2 \times 10^{-8}$, implying a completely laminar flow regime. Estimates of emplacement duration range from one to several decades. These new calculations confirm the unusual nature of these features and support previous qualitative suggestions that they were formed from magmas with significantly higher viscosity than those typical of mare basalts. *INDEX TERMS:* 5480 Planetology: Solid Surface Planets: Volcanism (8450); 5410 Planetology: Solid Surface Planets: Composition; 5460 Planetology: Solid Surface Planets: Physical properties of materials; 8429 Volcanology: Lava rheology and morphology; *KEYWORDS:* Moon, volcanism, domes

Citation: Wilson, L., and J. W. Head, Lunar Gruithuisen and Mairan domes: Rheology and mode of emplacement, *J. Geophys. Res.*, *108*(E2), 5012, doi:10.1029/2002JE001909, 2003.

1. Introduction

[2] The Gruithuisen and Mairan domes, located in northern Oceanus Procellarum (Figure 1), represent examples of topographically, morphologically and spectrally distinctive structures on the Moon [*Malin*, 1974; *Head and McCord*, 1978; *Chevrel et al.*, 1999; *Head and Wilson*, 1992, and references therein] that appear to be candidates for the sites of extrusion of very viscous magma about 3.7–3.85 Gyr ago [*Wagner et al.*, 2002]. In this analysis, we use the basic morphologic and morphometric characteristics of the domes as a basis for estimation of their yield strength, plastic viscosity, eruption rates, dike feeder geometry (e.g., dike width and length), and eruption duration. We then compare these values with those characterizing terrestrial environments and compositions.

2. Initial Estimates of Rheological Parameters

[3] The Gruithuisen and Mairan domes are sufficiently symmetrical that it is more appropriate to regard them as being the result of the extrusion of magma onto a flat plane, across which it spreads in all directions from the vent, than onto an inclined surface down which it flows in one main direction. Available treatments of such dome-forming eruptions are those of *Huppert* [1982], *Huppert et al.* [1982], *Blake* [1990], *Fink and Griffiths* [1990], and *Sakimoto and Zuber* [1995]. *Huppert* [1982] and *Huppert et al.* [1982] treated aspects of the motion of a Newtonian magma of constant viscosity and did not consider how cooling of the flow surface would limit the motion of such a flow. *Fink and Griffiths* [1990] considered cooling mainly in so far as it affected the development of surface textures on a flow rather than the rheology of the flow interior. *Sakimoto and Zuber* [1995] treated a Newtonian fluid with time-variable viscosity and showed that a sufficiently large increase in viscosity could effectively cause motion to cease; however their numerical treatment does not lend itself easily to modeling the dimensions of a dome produced by a given effusion rate. The most suitable model in this respect is that of *Blake* [1990], which treats the cooling magma as a Bingham plastic characterized by a yield strength, τ, and plastic viscosity, η. The yield strength is given by

$$\tau = \left(0.323\ d_{tot}^2 \rho\, g\right)/r_m \qquad (1)$$

where ρ is the lava density (we initially adopt 2000 kg/m^3 and discuss the reason for, and significance of, this later), g

0148-0227/03/2002JE001909$09.00

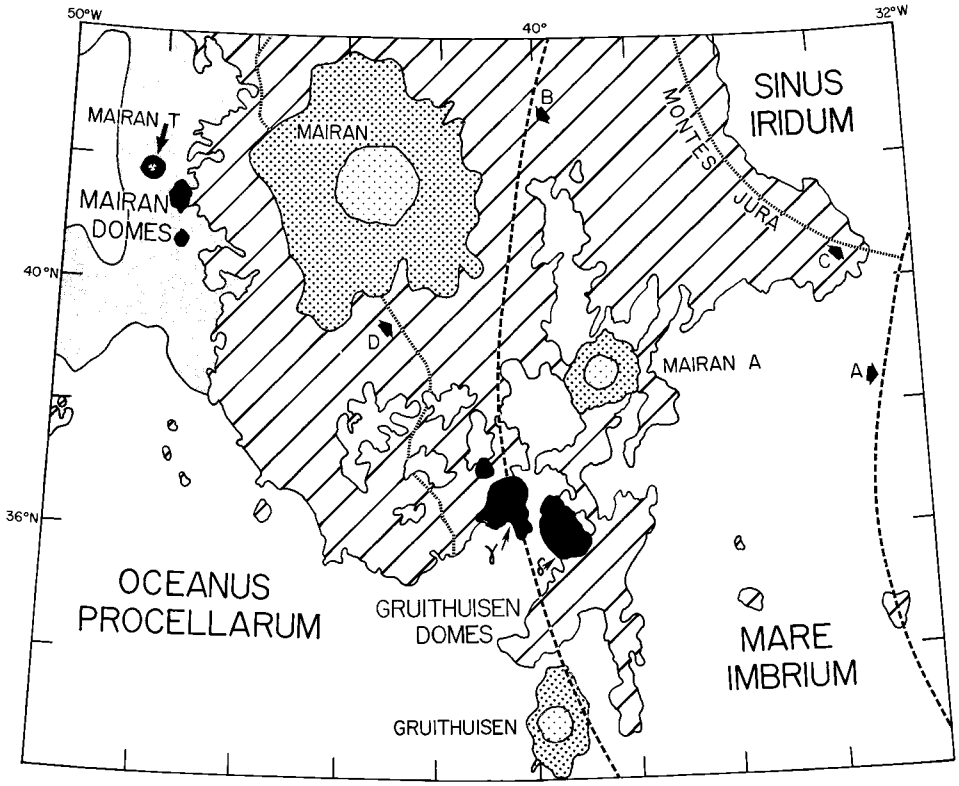

Figure 1. Location of the Gruithuisen and Mairan domes (black) and their geologic setting in northeastern Oceanus Procellarum and northwestern Mare Imbrium. The small dome to the northwest of Gruithuisen γ is the Gruithuisen Northwest (NW) dome. Traces of the location of the rings of the Imbrium multiringed basin are marked A and B, and the rim of the younger Iridum crater is marked C. Obliquely lined regions are highland material dominated by Iridum ejecta deposits. The line marked D denotes the change from radially textured ejecta toward Iridum to regions of secondary craters away from it. The mare units (plain pattern) flood and embay the uplands, and are mostly Imbrian in age. Eratosthenian mare units surrounding the Mairan domes are indicated in gray. Other impact craters have a stippled pattern. One degree of latitude equals about 30 km.

the acceleration due to gravity (1.63 m/s^2), r_m the radius of the dome and d_{tot} its maximum height. Table 1 gives the measured values of r_m and d_{tot}: we treat the Gruithuisen domes γ and NW and all three of the Mairan domes as being circular for this purpose and give the radial extent (i.e. the half-width) at right-angles to the long axis for the elongate dome Gruithuisen δ. Table 1 also gives the inferred values of τ. They are of order 3×10^5 Pa for the Gruithuisen domes and 1.0×10^5 Pa for the Mairan features, all larger than the values found for the distinctive festoon structure on Venus [*Head et al.*, 1992; *Pavri et al.*, 1992; *Moore et al.*, 1992; *Head and Hess*, 1996], mainly due to the greater thickness of the domes on the Moon.

[4] Next we use an empirical formula given by *Moore and Ackerman* [1989] to relate the plastic viscosity, η, to the yield strength, τ:

$$\eta(\tau) = Q\tau^{2.4} \quad (2)$$

where $Q = 6 \times 10^{-4}$ when η is expressed in Pa s and τ is in Pa. On this basis (see Table 1), the most likely value of η for the Gruithuisen domes is $\sim 1 \times 10^{10}$ Pa s and for the Mairan domes is within a factor of about two of 5×10^8 Pa s. The above analysis is oversimplified, however, in that all of the Gruithuisen domes show evidence for having been formed from more than a single flow unit. The δ and NW domes have very small secondary domes on top of the main dome and the γ dome has three flow lobes descending from near its summit [*Head et al.*, 1978] (Figure 2). We therefore analyze each of the major Gruithuisen domes in more detail in the following sections.

3. Analysis of the Gruithuisen γ Dome

[5] We treat this feature (Figure 1) as an underlying symmetric dome of radius r_m = 10 km and unknown thickness d_m on which are superimposed three flow lobes;

Table 1. Measured Values of the Maximum Radial Extent r_m and Total Thickness d_{tot} for All of the Domes Studied, and of the Implied Yield Strength τ and Plastic Viscosity, η, of the Material Forming the Domes

Dome Name	r_m/m	d_{tot}/m	τ/Pa	η/(Pa s)
Gruithuisen γ	10000	1200	1.5×10^5	1.6×10^9
Gruithuisen δ	6500	1550	3.9×10^5	15.6×10^9
Gruithuisen NW	4000	1100	3.2×10^5	9.7×10^9
Mairan T	6500	900	13.1×10^4	11.5×10^8
Mairan "middle"	5500	600	6.9×10^4	2.5×10^8
Mairan "south"	5000	500	5.3×10^4	1.3×10^8

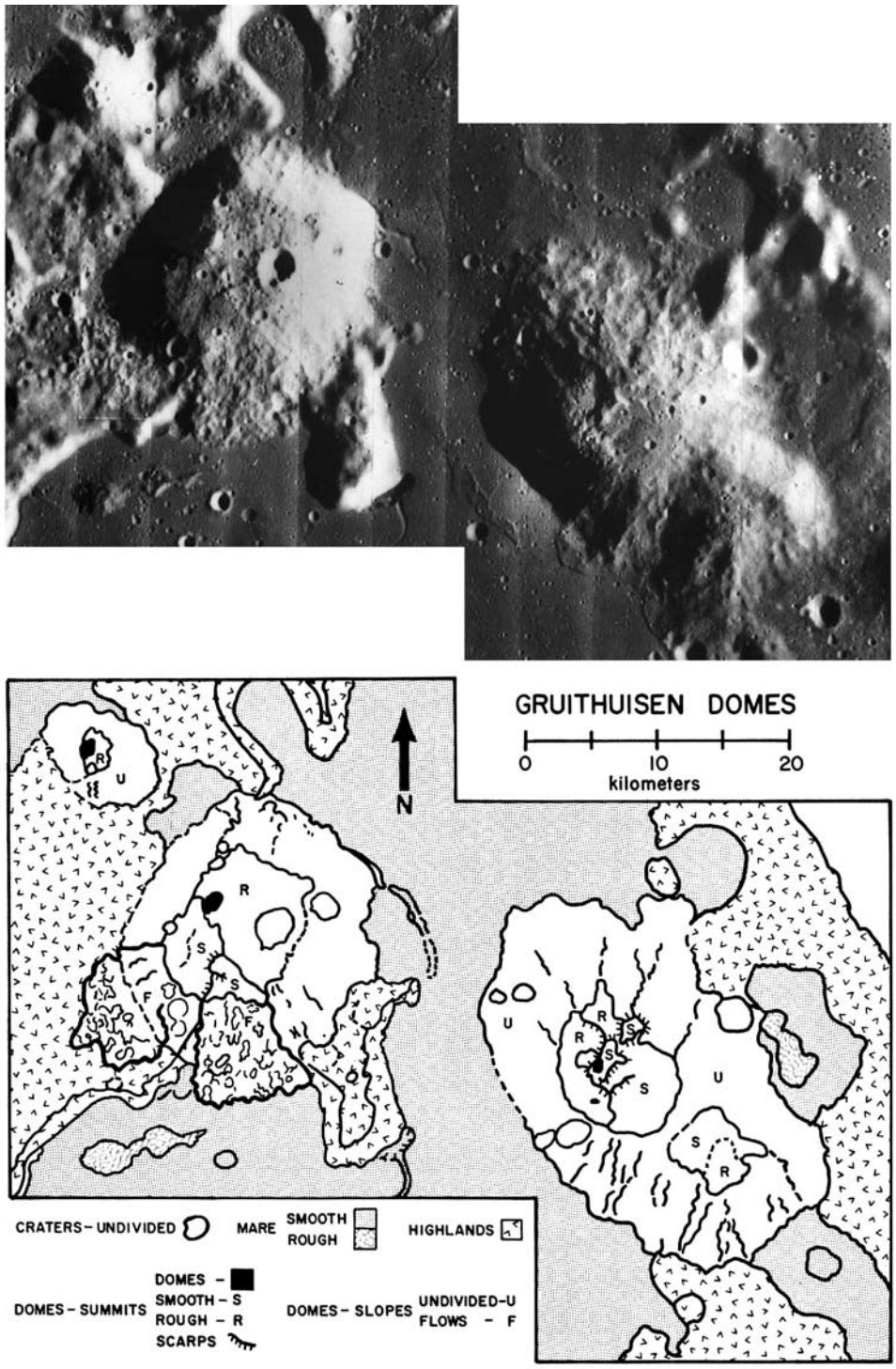

Figure 2. Top: Lunar Orbiter image of the Gruithuisen domes region (see Figure 1 for locations and context for domes). Portion of Lunar Orbiter IV 145 H1. Bottom: Geologic sketch map of the Gruithuisen domes [from *Head et al.*, 1978].

we assume that these merge toward the summit where they have a common thickness d_c. The observed apparent height of the dome, d_{tot} = 1200 m, is then the sum of d_m and d_c. The two flows which can be mapped in most detail (those to the southwest and south of the summit) both have total widths, w_t, of about 5 km where they descend the steeper parts of the dome slope. We treat both the underlying dome and the flows as Bingham plastics with the same rheological properties. Equation (1) still applies for the dome except that d_m (= $d_{tot} - d_c$) now has an unknown value less than 1200 m. *Hulme* [1974] showed that the center-line thickness, d_c, of a Bingham plastic flow lobe is given by

$$d_c^2 = (w_t \tau)/(\rho g) \quad (3)$$

Table 2. Measured Values of the Maximum Radial Extents, r_{ml} and r_{mu}, of the Lower and Upper Components, Respectively, of Two of the Gruithuisen Domes[a]

Dome Name	r_{ml}/m	r_{mu}/m	β/m	τ/Pa	d_{ml}/m	d_{mu}/m	η/(Pa s)
Gruithuisen δ (NW minor dome)	6500	4000	116.1	12.2×10^4	869	681	9.7×10^8
Gruithuisen δ (SE minor dome)	6500	2750	135.7	14.2×10^4	939	611	13.9×10^8
Gruithuisen NW	4000	1500	116.4	12.3×10^4	682	418	9.9×10^8

[a]See text for discussion. Also given are the value of β deduced from equation (7); the implied value of the yield strength τ from equation (8); the thicknesses, d_{ml} and d_{mu}, of the lower and upper domes implied by equation (9); and the plastic viscosity η deduced from τ via equation (2).

and is independent of the slope on which it is emplaced. We can rearrange this expression for the yield strength of the flow as $\tau = (\rho\, g\, d_c^2)/w_t$ and equate it to the value of τ for the dome given by equation (1) to obtain a quadratic equation in d_c which has the solution

$$d_c = d_{dot}\left[\left(\alpha^{0.5} - 1\right)/(\alpha - 1)\right] \quad (4)$$

where α is the value of $[r_m/(0.323\ w_t)]$. The measured values of $r_m = 10$ km and $w_t = 5000$ m lead to $\alpha = 6.192$, and so with $d_{tot} = 1200$ m we find $d_c = 344$ m. This means that $d_m = 1200 - 344 = 856$ m and equation (1) then implies $\tau = 7.7 \times 10^4$ Pa. Equation (2) then gives $\eta = 3.2 \times 10^8$ Pa s. These values are, as expected, significantly less than the first approximations given in Table 1 which ignored the detailed morphology of the dome.

4. Analysis of the Gruithuisen δ and NW Domes

[6] Each of these features (Figure 1) consists of a large dome on which is superimposed one (in the case of NW) or two (in the case of δ) smaller domes (Figure 2). Let the maximum radial extents of the larger, lower dome and the smaller, upper dome be r_{ml} and r_{mu}, respectively, and let their maximum thicknesses be correspondingly d_{ml} and d_{mu}. In the case of NW the radial distances are true radii since both upper and lower domes are essentially circular. In the case of δ, the underlying dome is strongly elongate and the two superimposed domes are less strongly elongate but with the same orientations: in these cases the "radial distances" are the half-widths measured at right angles to the long axis. The measured values are given in Table 2. For the lower dome in each case we can write the equivalent of equation (1):

$$\tau = \left(0.323\ d_{ml}^2 \rho\, g\right)/r_{ml} \quad (5)$$

and for the upper dome

$$\tau = \left(0.323\ d_{mu}^2 \rho\, g\right)/r_{mu} \quad (6)$$

where we assume, as before, that both domes are made of material with the same rheological properties. The sum of d_{ml} and d_{mu} is the total measured height of the composite dome, d_{tot}, and so we can use the above expression for d_{ml} and d_{mu} to give

$$d_{tot} = \beta^{0.5}\left(r_{ml}^{0.5} + r_{mu}^{0.5}\right) \quad (7)$$

where β is defined by

$$\beta = \tau/(0.323\ \rho\, g) \quad (8)$$

and it follows that

$$\left(d_{ml}^2/r_{ml}\right) = \left(d_{mu}^2/r_{mu}\right) = \beta \quad (9)$$

[7] Table 2 shows the values of β found for each pair of domes by inserting the total thickness d_{tot} (from Table 1) and the measured values of r_{ml} and r_{mu} into equation (7). Also given are the implied values of τ from equation (8) and the corresponding values of d_{ml} and d_{mu} from equation (9) and the plastic viscosity η implied by equation (2). As was the case for the Gruithuisen γ dome, the values found for the rheological parameters are smaller than the first approximations given in Table 1.

5. Summary of Rheological Parameters

[8] In Table 3 we show the values found for τ and η by the various methods of analysis employed so far. Given the resolution of the images used and the consequent difficulties in mapping and measuring features, it might be argued that all of these measurements represent a single Bingham plastic magma for which $\tau = (10 \pm 3) \times 10^4$ Pa and $\eta = (6 \pm 4) \times 10^8$ Pa s. Alternatively we could separate the two groups of domes and characterize the Gruithuisen dome magma by $\tau = (12 \pm 3) \times 10^4$ Pa, $\eta = (10 \pm 5) \times 10^8$ Pa s

Table 3. Summary of the Values of Yield Strength τ and Plastic Viscosity η Found for the Domes Studied Using Various Methods

Dome Name	Method Used	τ/Pa	η/(Pa s)
Gruithuisen γ	flows superposed on dome	7.7×10^4	3.2×10^8
Gruithuisen δ (NW)	two superposed domes	12.2×10^4	9.7×10^8
Gruithuisen δ (SE)	two superposed domes	14.2×10^4	13.9×10^8
Gruithuisen NW	two superposed domes	12.3×10^4	9.9×10^8
Mairan T	single dome	13.1×10^4	11.5×10^8
Mairan "middle"	single dome	6.9×10^4	2.5×10^8
Mairan "south"	single dome	5.3×10^4	1.3×10^8

Table 4. Summary of the Radii, r_m, and Thicknesses, d_m, of the Various Dome Components and the Implied Volume Eruption Rates, E, of Magma if the Flow Units Are Cooling Limited

Dome Name	r_m/m	d_m/m	E/(m^3/s)
Gruithuisen γ	10000	856	119.3
Gruithuisen δ (NW lower dome)	6500	869	49.7
Gruithuisen δ (NW upper dome)	4000	681	24.0
Gruithuisen δ (SE lower dome)	6500	939	46.0
Gruithuisen δ (SE upper dome)	2750	611	12.6
Gruithuisen NW (lower dome)	4000	682	24.0
Gruithuisen NW (upper dome)	1500	418	5.5
Mairan T	6500	900	48.0
Mairan "middle"	5500	600	51.5
Mairan "south"	5000	500	51.1

and the Mairan dome magma by the slightly smaller values $\tau = (8 \pm 4) \times 10^4$ Pa, $\eta = (5 \pm 4) \times 10^8$ Pa s.

6. Eruption Rate Estimates

[9] We now turn to the estimation of the eruption rates of the magmas forming the various dome units. To do this we assume that the advance of the flow front of each flow unit or dome-forming episode was limited by cooling. *Pinkerton and Wilson* [1994] show that a variety of types of lava flows cease to move when the Grätz number, a dimensionless measure of the depth of penetration into the flow of the cooled boundary layer, has decreased from its initially very high value to a critical value of about 300. This is shown to correspond to assuming that the flow has been moving for a time T such that

$$T = d_f^2/(300\,\kappa) \tag{10}$$

where κ is the thermal diffusivity of the lava ($\sim 10^{-6}$ m^2/s) and d_f is the thickness of the flow near its front.

[10] *Blake*'s [1990] model of Bingham plastic domes shows that the radius of the dome, r, grows as a function of time, t, given by

$$r = 0.65\left[\left(E^2 \rho\, g\right)/\tau\right]^{1/5} t^{2/5} \tag{11}$$

where E is the volume eruption rate. For a symmetrical dome, it is not trivial to define the thickness d_f which corresponds to the distal thickness of a lava flow lobe. We assume that a reasonable approximation is to take the thickness of the dome halfway between its center and its edge. The parabolic dome profiles implied by *Blake*'s [1990, equation (23)] model are

Table 5. Values of the Total Levee Width, ($2\,w_b$), the Width of the Channel in Which Lava Flowed, w_c, and the Implied Volume Eruption Rate of Magma, E, for the Southwest Flow Lobe on the Flank of Gruithuisen γ, Calculated for a Series of Assumed Values of sin ϑ for the Flank Slope

sin ϑ	($2\,w_b$)/m	w_c/m	E/(m^3/s)
0.125	1512	3488	5407
0.100	2362	2638	1795
0.090	2916	2084	801
0.085	3269	1731	441
0.080	3691	1309	187
0.075	4199	801	44

Table 6. Values of Mean Dike Width, W, Horizontal Dike Length, L, Magma Rise Speed, U, and Reynolds Number of Magma Motion, Re, as a Function of Magma Density, ρ, for Magma Feeding Dome Eruptions at a Fixed Volume Flux of 50 m^3 s^{-1}

ρ/(kg m^{-3})	W/m	L/km	U/(m s^{-1})	Re
2400	307	61	3×10^{-6}	0.5×10^{-8}
2000	154	33	11×10^{-6}	1.0×10^{-9}
1600	103	21	24×10^{-6}	1.6×10^{-9}

such that d_f defined in this way is equal to $\sim 0.7 d_m$. Substituting this relationship and equation (10) into equation (11) we obtain an expression relating the radius of the dome when it ceases spreading (i.e. r_m) to its maximum thickness at this time, d_m, and the effusion rate feeding it:

$$r_m = 0.65\ 0.7^{4/5} 300^{-2/5} \left[\left(E^2 \rho\, g\right)/\left(\tau \kappa^2\right)\right]^{1/5} {d_m}^{4/5}. \tag{12}$$

Eliminating τ from this equation using equation (1) and rearranging:

$$E = \left[\left(0.323^{1/2}\ 300\ \kappa {r_m}^2\right)/\left(0.65^{5/2} 0.72\ d_m\right)\right]. \tag{13}$$

Table 4 summarizes the values of r_m and d_m for all of the dome components and the values of effusion rate that they imply. It must be pointed out that the assumption that flow lobes are cooling-limited always leads to effusion rate estimates that are lower bounds. This is because any flow unit assumed to be cooling-limited may in fact have been volume-limited (i.e. ceased to flow simply because the magma supply was exhausted), implying that it had the potential to travel further than the observed distance and therefore had a higher effusion rate than that deduced. For each of the Gruithuisen domes (Figures 1 and 2) we have either a second smaller dome or a flow lobe superimposed on a larger, earlier dome. It is very tempting to assume that the second unit in each case is a break-out at the vent caused by the magma supply continuing after the first unit has reached its cooling-limited length. This automatically implies that the effusion rates deduced from the large dome geometries ($\sim$48, 24 and 119 m^3/s for Gruithuisen δ, NW and γ, respectively) are the realistic estimates and that the rates found from the smaller units are underestimates. For the Mairan domes we are not able to resolve multiple lobe structures and must regard the (as it happens remarkably similar) effusion rates of $\sim$50 m^3/s as lower limits on the true rates.

[11] It is possible to obtain useful information by considering the motion of the flow lobes on the flanks of Gruithuisen γ. The relevant theory is outlined by *Hulme* [1974]: a Bingham plastic flow with total width w_t emplaced on a plane inclined at an angle ϑ to the horizontal has stationary margin levees of width w_b such that

$$2w_b = \tau/\left(\rho\, g \sin^2 \vartheta\right). \tag{14}$$

The width of the channel within which lava moves is then $w_c = w_t - 2w_b$. This channel width can be related to the other variables, including the effusion rate E, by

$$(24\ \eta E)^4 = \left({w_c}^{11} \tau^5 \sin^6 \vartheta\right)/(\rho\, g) \tag{15}$$

Table 7. Values of the Best Estimates of Yield Strength, τ, Plastic Viscosity, η, and Volume Eruption Rate, E, for Each of the Domes and of the Corresponding Values Calculated for the Width, W, and Length, L, of the Underlying Feeder Dike[a]

Feature	τ/Pa	η/(Pa s)	E/(m^3/s)	W/m	L/km	L_e/km
Gruithuisen γ	7.7×10^4	3.2×10^8	119	119	24	5–10
Gruithuisen δ	13.2×10^4	11.8×10^8	48	203	41	12–15
Gruithuisen NW	12.3×10^4	9.9×10^8	24	189	38	2–3
Gruithuisen NW and γ combined	10.0×10^4	6.0×10^8	143	154	31	18–20
Mairan T	13.1×10^4	11.5×10^8	24	201	40	1–2
Mairan "middle"	6.9×10^4	2.5×10^8	52	106	21	2–3
Mairan "south"	5.3×10^4	1.3×10^8	51	82	16	~1
Mairan "middle" and "south" combined	6.1×10^4	1.8×10^8	52	94	19	8–10

[a]An estimate of the dike length, Le, obtained from the interpretation of the images is included for comparison.

which is a slight simplification of Hulme's original formula suggested by *Wilson and Head* [1983]. Table 5 gives examples of the solution of equations (14) and (15) using our estimate of 5 km for w_t and a range of plausible values of sin ϑ. The range is chosen to encompass the mean slope of the flanks of the underlying dome which, for the shallow angles involved, is of order sin $\vartheta \cong \tan \vartheta \cong$ (856 m/10 km) $\cong 0.085$. The analysis clearly suggests that E is ~400 m^3/s, which is not greatly at variance with the 119 m^3/s deduced by applying the cooling-limited criterion to the underlying dome. However, because of the strong dependence of E on the values used for sin ϑ and w_c, this estimate must be regarded as very inaccurate: if 6 km were adopted for w_t instead of the 5 km used above, the estimate of E would increase by a factor of more than three.

7. Geometries of Feeder Dikes

[12] To explore the conditions under which the magmas erupted we assume that in each case the melt reached the surface from a source region at least as deep as the base of the mainly anorthositic crust. Assuming a mean crustal density $\rho_c = 2800$ kg/m^3 and recalling the assumed magma density of $\rho = 2000$ kg/m^3, the pressure gradient driving the magma rise is $\sim[g(\rho_c - \rho)] = \sim 130$ Pa m^{-1}. The magma rise speed is found by balancing the driving pressure gradient against the wall friction which, allowing for the need to overcome the yield strength, leads to [*Wilson and Head*, 1981; *Johnson and Pollard*, 1973]

$$U = \left[W^2/(12\eta)\right][g(\rho_c - \rho) - (2\tau/W)] \quad (16)$$

The rise speed, dike geometry and volume eruption rate are related by

$$E = U\,W\,L. \quad (17)$$

but horizontal length L and width W of the dike are not independent; their ratio is a function of the elastic and plastic properties of the crustal rocks and also of the viscosity of the magma. *Rubin* [1993] showed that for magmas with the relatively high viscosity found here, and assuming a mean viscosity of $\sim 10^{18}$ Pa s for the hot lower crustal rocks through which the dike passes, the ratio L/W probably lies within a factor of 2 of 200. Using this value and combining the above expressions, we have

$$W^4 = [(12\,\eta E)/200]/[g(\rho_c - \rho) - (2\tau/W)] \quad (18)$$

from which W can be obtained recursively from any initial estimate.

[13] Using the mean rheological properties for all of the domes, $\tau = 10 \times 10^4$ Pa and $\eta = 6 \times 10^8$ Pa s, together with an eruption rate of 50 m^3/s (typical of the majority of the values in Table 4), we find W = 154 m and so L = 31 km. The magma rise speed implied by this geometry is very small, 11×10^{-6} m/s, and the Reynolds number of the motion is $\sim 10^{-8}$, implying a completely laminar flow regime. At first sight the implied fissure length of ~30 km seems large judged against the facts that (i) the δ dome is elongate with its main vents ~12 km apart and (ii) the γ and NW domes together could be regarded as defining an underlying fissure about 18 km long (Figures 1 and 2). However, it is common on Earth for eruptions to localize so that only part of an initial fissure remain active throughout an eruption [*Richter et al.*, 1970; *Wolfe et al.*, 1988; *Wilson and Head*, 1988].

[14] We have repeated the solution of equation (18) with a range of magma densities. Increasing the magma density (i.e. reducing the buoyancy) makes U smaller and W and L larger. Table 6 shows the results of using $\rho = 2400$, 2000 and 1600 kg m^{-3}. The solutions W = 103 m and L = ~21 km, found for the very small magma density of 1600 kg m^{-3}, imply a dike length close to that evidenced by the observations. Thus, one possible explanation for the unusual properties of the magma involved in building these domes is that it is an extremely vesicular foam.

[15] In order to see if a better fit to the inferred dike geometries can be found, we give in Table 7 the individual best estimates of τ, η and E for each of the domes, the corresponding calculated values of W and L using the

Table 8. Summary of the Key Values for the Gruithuisen and Mairan Domes[a]

Dome Name	r_m/m	d_m/m	V/km^3	E/(m^3/s)	D/years
Gruithuisen γ	10000	856	135.9	119.3	38.0
Gruithuisen δ (NW lower dome)	6500	869	57.7	49.7	38.7
Gruithuisen δ (NW upper dome)	4000	681	17.1	24.0	23.8
Gruithuisen δ (SE lower dome)	6500	939	62.3	46.0	45.1
Gruithuisen δ (SE upper dome)	2750	611	7.3	12.6	19.3
Gruithuisen NW (lower dome)	4000	682	17.1	24.0	23.8
Gruithuisen NW (upper dome)	1500	418	1.5	5.5	9.1
Mairan T	6500	900	59.7	48.0	41.5
Mairan "middle"	5500	600	28.5	51.5	18.4
Mairan "south"	5000	500	19.6	51.1	12.8

[a]Values include dome radii, r_m, heights, d_m, volumes, V (treating the domes as parabolas so that $V = [(\pi/2)\, r_m^2\, d_m]$), effusion rates, E, and the implied duration of formation, D, equal to (V/E).

original magma density estimate of 2000 kg/m^3, and for comparison the estimates of active fissure length L_e based on the morphology and arrangement of the domes. Examination of this table confirms that it is plausible to assume that Gruithuisen NW and Gruithuisen γ are fed by the same dike. It also seems likely that Mairan "middle" and Mairan "south" share a common feeder. However, Mairan T appears to be anomalous in respect of the geometry of the dike needed to supply it. Indeed, Mairan T appears to be significantly different from Mairan "middle" and Mairan "south" in terms of its rheological properties, largely as a result of its large thickness to diameter ratio, and it seems likely that it, like the Gruithuisen domes, is a composite feature. If Mairan T consists of two phases of extrusion which produced domes with radii 6500 (the mapped radius) and 3000 m (an arbitrary but plausible value), the superposed dome treatment used earlier would yield $\beta = 44.2$ m, $\tau = 4.7 \times 10^4$ Pa and $\eta = 1.0 \times 10^8$ Pa s; the implied effusion rate for the main phase would be 81 m^3/s, and the width and length of the feeding dike would be 72 m and 14 km, respectively. This value of the dike length is much more consistent with the observed geometry of this dome.

8. Discussion and Conclusions

[16] In summary, we find typical values of yield strength, τ, of order 10^5 Pa, plastic viscosity, η, of order 10^9 Pa s, and effusion rate, E, of order 50 m^3/s. What do these values mean? Values of $\tau \sim 3 \times 10^5$ occur with terrestrial rhyolites, dacites and basaltic andesites [see *Blake*, 1990, Table 3]. Effusion rate values of up to 10 m^3/s for the Mt. St. Helens dacite dome lobes [*Anderson and Fink*, 1992], and about 5 m^3/s for the Soufriere basaltic andesite [*Blake*, 1990; *Huppert et al.*, 1982] have been documented.

[17] Typical dike geometries are predicted to be of width $\sim$100–200 m and length about 20–40 km. The magma rise speed implied by this geometry is very low, $\sim 10^{-5}$ m/s, and the Reynolds number of the motion is $\sim 10^{-8}$, implying a completely laminar flow regime. If the viscosity/yield strength relationship is unreliable, the W and L values will not be very reliable (though W depends on η raised to a power close to one quarter so this will not change the values dramatically). Total duration of formation of the domes can be estimated by using the data on effusion rates and volumes (Table 8). The range of formation times is estimated to be $\sim$10 to 50 years.

[18] In summary, these new calculations confirm the unusual nature of these features and support previous qualitative suggestions that they were formed from magmas with significantly higher viscosity than typical of mare basalts.

[19] **Acknowledgments.** This work was support by a grant to J.W.H. from the NASA Planetary Geology and Geophysics Program. Thanks are extended to B. Ray Hawke for a critical review.

References

Anderson, S. W., and J. H. Fink, Crease structures: Indicators of emplacement rates and surface stress regimes of lava flows, *Geol. Soc. Am. Bull.*, *104*, 615–625, 1992.

Blake, S., Viscoplastic models of lava domes, in *Lava Flows and Domes: Emplacement Mechanisms and Hazard Implications*, *IAVCEI Proc. Volcanol.*, vol. 2, edited by J. Fink, pp. 88–128, Springer-Verlag, New York, 1990.

Chevrel, S., P. C. Pinet, and J. W. Head, Gruithuisen domes region: A candidate for an extended nonmare volcanism unit on the Moon, *J. Geophys. Res.*, *104*, 16,515–16,529, 1999.

Fink, J. H., and R. W. Griffiths, Radial spreading of viscous-gravity currents with solidifying crust, *J. Fluid Mech.*, *221*, 485–509, 1990.

Head, J. W., and P. C. Hess, Formation of tertiary crust on Venus by remelting of tessera crustal roots: The Ovda Regio festoon, *Lunar Planet. Sci.*, *27*, 513–514, 1996.

Head, J. W., and T. B. McCord, Imbrian-aged highland volcanism on the Moon, The Gruithuisen and Marian domes, *Science*, *199*, 1433–1436, 1978.

Head, J. W., and L. Wilson, Lunar mare volcanism: Stratigraphy, eruption conditions, and the evolution of secondary crusts, *Geochim. Cosmochim. Acta*, *55*, 2155–2175, 1992.

Head, J. W., P. C. Hess, and T. B. McCord, Geologic characteristics of lunar highland volcanic domes (Gruithuisen and Mairan region) and possible eruption conditions, *Proc. Lunar Planet. Sci. Conf.*, *9th*, 488–490, 1978.

Head, J. W., L. S. Crumpler, J. C. Aubele, J. Guest, and R. S. Saunders, Venus volcanism: Classification of volcanic features and structures, associations, and global distribution from Magellan data, *J. Geophys. Res.*, *97*(E8), 13,153–13,197, 1992.

Hulme, G., The interpretation of lava flow morphology, *Geophys. J. R. Astron. Soc.*, *39*, 361–383, 1974.

Huppert, H. E., The propagation of two-dimensional and axisymmetric viscous gravity currents over a rigid horizontal surface, *J. Fluid Mech.*, *188*, 107–131, 1982.

Huppert, H. E., J. B. Shepherd, H. Sigurdsson, and R. S. J. Sparks, On lava dome growth, with application to the 1979 lava extrusion of the Soufrière of St. Vincent, *J. Volcanol. Geotherm. Res.*, *14*, 199–222, 1982.

Johnson, A. M., and D. D. Pollard, Mechanics of growth of some laccolithic intrusions in the Henry Mountains, Utah, I, Field observations, Gilbert's model, physical properties and flow of the magma, *Tectonophysics*, *18*, 261–309, 1973.

Malin, M., Lunar red spots: Possible pre-mare materials, *Earth Planet. Sci. Lett.*, *21*, 331–341, 1974.

Moore, H. J., and J. A. Ackerman, Martian and terrestrial lava flows, in *Reports on Planetary Geology Geophysics Program-1988*, *NASA Tech. Memo. TM-4130*, 387–389, 1989.

Moore, H. J., J. J. Plaut, P. M. Schenk, and J. W. Head, An unusual volcano on Venus, *J. Geophys. Res.*, *97*(E8), 13,479–13,493, 1992.

Pavri, B., J. W. Head, K. B. Klose, and L. Wilson, Steep-sided domes on Venus: Characteristics, geologic setting, and eruption conditions from Magellan data, *J. Geophys. Res.*, *97*(E8), 13,445–13,478, 1992.

Pinkerton, H., and L. Wilson, m Factors controlling the lengths of channel-fed lava flows, *Bull. Volcanol.*, *56*, 108–120, 1994.

Richter, D. H., J. P. Eaton, K. J. Murata, W. H. Ault, and H. L. Krivoy, Chronological narrative of the 1959–60 eruption of Kilauea volcano, Hawaii, *U. S. Geol. Surv. Prof. Pap.*, *537-E*, 1–73, 1970.

Rubin, A. M., Dikes vs. diapirs in viscoelastic rock, *Earth Planet. Sci. Lett.*, *119*, 641–659, 1993.

Sakimoto, S., and M. T. Zuber, Effects of planetary thermal structure on the ascent and cooling of magma on Venus, *J. Volcanol. Geotherm. Res.*, *64*, 53–60, 1995.

Wagner, R., J. W. Head III, U. Wolf, and G. Neukum, Stratigraphic sequence and ages of volcanic units in the Gruithuisen region of the Moon, *J. Geophys. Res.*, *107*(E11), 5104, doi:10.1029/2002JE001844, 2002.

Wilson, L., and J. W. Head, Ascent and eruption of basaltic magma on the Earth and Moon, *J. Geophys. Res.*, *86*(B4), 2971–3001, 1981.

Wilson, L., and J. W. Head, A comparison of volcanic eruption processes on Earth, Moon, Mars, Io and Venus, *Nature*, *302*, 663–669, 1983.

Wilson, L., and J. W. Head, Nature of local magma storage zones and geometry of conduit systems below basaltic eruption sites: Pu'u O'o, Kilauea, East Rift, Hawaii example, *J. Geophys. Res.*, *93*(B12), 14,785–14,792, 1988.

Wolfe, E. W., C. A. Neal, N. G. Banks, and T. J. Duggan, Geological observations and chronology of eruptive events, in *The Puu Oo Eruption of Kilauea Volcano, Hawaii; Episodes 1 Through 20, January 3, 1983, Through June 8, 1984*, *U. S. Geol. Surv. Prof. Pap.*, *1463*, 1–97, 1988.

J. W. Head, Department of Geological Sciences, Brown University, Providence, RI 02912, USA. (james_head_III@brown.edu)

L. Wilson, Environmental Science Department, Lancaster University, Lancaster, LA1 4YQ, UK.